

On the relativistic origin of the kink effect in the chain of Pb isotopes

S. Marcos^a, L.N. Savushkin^b, M. López-Quelle^c, R. Niembro^a, P. Bernardos^d

^a *Departamento de Física Moderna, Universidad de Cantabria, E-39005 Santander, Spain*

^b *Department of Physics,*

St. Petersburg University for Telecommunications, 191065 St. Petersburg, Russia

^c *Departamento de Física Aplicada, Universidad de Cantabria, E-39005 Santander, Spain*

^d *Departamento de Matemática Aplicada y Ciencias de la Computación,*

Universidad de Cantabria, E-39005 Santander, Spain

(November 28, 2018)

Abstract

We investigate the origin of the kink effect (KE) in the relativistic mean field theory by transforming the single-particle Dirac equation into a Schrödinger-like equation. It is found that relativistic self-consistent effects as well as contributions coming from the ρ meson determine the actual structure of the KE. However, the spin-orbit force generated by the ρ meson has no significant influence on the KE.

PACS numbers: 21.30.+y, 21.10.Ft, 21.60.Jz

The charge radii (r_c) of the Pb isotopes have been measured a few years ago with a very high precision [1], their anomalous kink behavior being the most essential feature of these measurements. The kink effect (KE) means that the experimental data on r_c as a function of A in the isotopic chain display a change of the slope at N=126 with a gradual addition of neutrons. This phenomenon has been a matter of a detailed discussion by different theoretical groups during the recent years (see Refs. [2]- [6] and references therein).

At the first stage, it has been shown that the density-dependent Hartree-Fock model with standard parametrizations of the Skyrme (SHF) [2] or Gogny [7] forces fails to reproduce the empirical charge isotopic shifts in the chain of Pb isotopes.

On the other hand, in Refs. [3,4] the anomalous behavior of the charge radii of these isotopes has been studied in the relativistic mean field approach (RMFA). The Pb data are well described by this type of theory. In Ref. [4] it is supposed that the success of the RMFA in reproducing the KE is achieved due to the weak isovector dependence of the spin-orbit force generated by the RMFA.

In Ref. [5] the problem of isotopic shifts has been investigated with exhaustive detail, both in the SHF and RMFA. The authors of Ref. [5] have proposed a new Skyrme functional SkI4 with a more general structure of the spin-orbit force than that of the standard Skyrme functional. They have also succeeded to reproduce the KE, but at the price of introducing an extra parameter for the two body spin-orbit potential.

As the authors of Refs. [3,4] state, the standard RMFA provides an excellent description of the anomalous kink in the isotopic shifts about ^{208}Pb without using extra fitting parameters. In the present paper we shall focus our interest into the problem of the origin of the KE in the RMFA paying special attention to the role of the isovector ρ meson in the kink structure.

In the RMFA [6], the relativistic single-nucleon wave function $\psi(\vec{r})$, for a nucleon with the rest mass M, satisfies the Dirac equation

$$[-i\hbar\vec{\alpha} \cdot \vec{\nabla} + \beta(M + S(\vec{r})) + V(\vec{r})]\psi(\vec{r}) = E\psi(\vec{r}), \quad (1)$$

where $E = M + \varepsilon$ and ε is the binding energy eigenvalue while $S(\vec{r})$ and $V(\vec{r})$ are the scalar and vector potentials, respectively, defined as follows:

$$S(\vec{r}) = g_\sigma \sigma(\vec{r}),$$

$$V(\vec{r}) = V_\omega(\vec{r}) + \tau_0 V_\rho(\vec{r}) + \frac{1 + \tau_0}{2} V_c(\vec{r}) = g_\omega \omega_0(\vec{r}) + \tau_0 g_\rho \rho_0(\vec{r}) + e \frac{1 + \tau_0}{2} A_0(\vec{r}). \quad (2)$$

In Eq. (2) σ is the scalar meson field, ω_0 and ρ_0 are the time components of the ω and ρ meson fields, respectively, while V_c is the Coulomb potential. g_σ , g_ω and g_ρ are the coupling constants associated with the respective mesons. All meson fields satisfy the corresponding Klein-Gordon equations (see [6], for example).

Eq. (1) can be reduced to a Schrödinger-like equation [8] which does not contain the first derivative of the wave function $[\tilde{\phi}(\vec{r})]$. It reads:

$$\left[-\frac{\hbar^2}{2M}\nabla^2 + V_{cent}(\vec{r}) + V_{SO}(\vec{r})\right]\tilde{\phi}(\vec{r}) = \varepsilon\left(1 + \frac{\varepsilon}{2M}\right)\tilde{\phi}(\vec{r}), \quad (3)$$

where the central potential V_{cent} and the spin-orbit potential V_{SO} are given by:

$$V_{cent}(\vec{r}) = S + V + \frac{S^2 - V^2}{2M} + \varepsilon\frac{V}{M} + \Delta V_{cent}, \quad (4)$$

$$\Delta V_{cent} = \frac{\hbar^2}{2M}\left[\frac{1}{4}W^2 + \frac{1}{r}W + \frac{1}{2}W'\right],$$

$$W = -\frac{S' - V'}{2M + \varepsilon + S - V};$$

$$V_{SO}(\vec{r}) = \frac{\hbar^2}{2M}\frac{2}{r}W\vec{l} \cdot \vec{s}. \quad (5)$$

By writing the Dirac equation in this form, we are able to study separately the influence of the different terms entering Eq. (4) on the KE (we can analyze, for example, if their respective effects are of relativistic origin or not).

Our calculations have been carried out for the *Pb* chain of isotopes around the ^{208}Pb nucleus in the framework of the standard RMFA, with a linear model (L) [9] and two nonlinear models NL-SH [10] and NL3 [11] containing self-interactions of the scalar field. For simplicity, we shall mainly concentrate our discussion in the three Pb isotopes ^{206}Pb , ^{208}Pb and ^{210}Pb . The most stable configuration of the ^{210}Pb isotope in the two nonlinear models considered contains two neutrons in the $1i_{11/2}$ states. In the L model, the two configurations in which two neutrons fill up the $1i_{11/2}$ or $2g_{9/2}$ single-particle states are almost degenerate (we shall refer to these two configurations as IC and GC, respectively). We approach the ^{210}Pb ground state by the IC in both linear and nonlinear models, although the BCS formalism would be more appropriate in the first case. Nevertheless, we expect that our conclusions are also valid for the L model, at least, at a qualitative level.

The self-consistent results for the charge radii corresponding to the exact models are summarized in Table I, case *a*, and in Fig. 1 (the r_c are normalized in this figure to the

experimental value of the ^{208}Pb nucleus). The KE appears in the three models considered but it is more strongly pronounced in models with smaller K modulus values. We notice that the KE is quite small for the GC, in spite of the fact that the $2g_{9/2}$ state is less bound than the $1i_{11/2}$ state and that the radius of the $2g_{9/2}$ state is larger than the radius of the $1i_{11/2}$ one. Thus, it is not the radius but the different neutron density associated with these two states that is essential to explain the different KE corresponding to IC and GC. The KE in the chain of Pb isotopes can be only explained if single-particle configurations including $1i_{11/2}$ states significantly contribute to the total nuclear ground state for the isotopes with $A > 208$.

To understand how the kink is generated by the model we have begun from studying the influence of the different mesons on the KE. We have calculated the r.m.s. radii of different components of the single-particle potential: S , V_ω and V_ρ as functions of the number A , and we have established that it is only the value of r_ρ , i.e., the r.m.s. radius of the ρ meson potential V_ρ , that shows a pronounced kink while the other components do not. Since the ρ meson has an isovector character, we can expect that it plays a relevant role in the behavior of protons when neutrons are added to the nucleus. Thus, the result mentioned above confirms the relevant role of the ρ meson in generating the KE.

Let us underline that the ρ meson contribution reveals itself in Eq. (4) in different terms of the total potential $V_{cent}(\varepsilon) + V_{SO}(\varepsilon)$ through the V component. Since the coupling constant g_ρ of the ρ meson is comparatively small, the most essential contribution of the ρ meson to the total potential comes from the $(S+V)$ and $(S^2 - V^2)/2M$ terms, where the σ and ω contributions cancel each other to a certain extent.

To study the influence of the different components containing the ρ meson field on the charge radii of the nuclei in more detail, it is useful to make the following replacements in eqs. (4) and (5) corresponding to $V_{cent}(\vec{r})$ and $V_{SO}(\vec{r})$, respectively : $g_\rho \rightarrow x_1 g_\rho$ in the $(S+V)$ term, $g_\rho \rightarrow x_2 g_\rho$ in the $(S^2 - V^2)/2M$ term, $g_\rho \rightarrow x_3 g_\rho$ in the $\frac{\varepsilon}{M}V$ term, $g_\rho \rightarrow x_4 g_\rho$ in the ΔV_{cent} term, and $g_\rho \rightarrow x_5 g_\rho$ in the V_{SO} potential. After that, we allow the parameters x_{1-5} to vary in a continuous and independent way in the interval $[0-1]$. We have considered 4 different cases corresponding to the 4 following combinations of the x_i parameters: *a*) $x_{1-5} = 1$ (already discussed) *b*) $x_1 \ll 1$, $x_{2-5} = 1$, *c*) $x_{1,3-5} = 1$, $x_2 = 0$, and *d*) $x_{1-5} = 0$ (equivalent to take $g_\rho = 0$).

The results for these cases are collected in Table I, and can be identified by the corresponding letter *a*, *b*, *c* or *d* in the last column. We have considered the models L, NL-SH and NL3, and the IC for the ground state. Fig. 2 shows the r_c results for the NL-SH model normalized to the r_c of the ^{208}Pb nucleus. The case *a* contains the total

ρ contribution and manifests the KE in good agreement with the effect experimentally observed. In the case *b*, in which the ρ contribution to $S + V$ is almost eliminated, the kink has completely changed its structure in relation to the case *a*, now the kink seems to be, somehow, the mirror image of the kink in case *a*. This fact makes evident the crucial role the ρ meson plays in the kink structure through the contribution of the $(S + V)$ term.

Table I shows that r_c slightly increases when the parameter x_1 decreases. This fact is related to the decreasing of the proton binding energy with the decreasing of the x_1 value (the opposite is true for the neutron energy). However the qualitative change of the kink structure cannot be attributed to this modification of r_c (which has only a small effect on the kink). Notice also that x_1 is taken equal to 0.2 and 0.1 (rather than 0) in the L and NL-SH models, respectively, to maintain the $3s_{1/2}$ proton state bound enough.

The effect of the ρ meson on the kink in the region $208 \leq A \leq 210$ through the term $S + V$ in the potential is quite small for the more stable IC. However, for the GC, a decreasing of the x_1 parameter produces a sizable turn at the left side of this region of the kink.

With regard to the case *c* in Fig. 2, the effect displayed is opposite to that shown in the case *b* and much smaller in magnitude. This result is a consequence of the opposite role the ρ meson field plays in the terms $(S + V)$ and $(S^2 - V^2)/2M$ of the central potential. For the GC the effect of the ρ meson on the kink through these two terms remains opposite to the case *b*, but comparable in magnitude.

Finally, for the case *d*, i.e., the case without ρ meson contribution, the behavior of r_c is intermediate between that corresponding to the cases *a* and *b* as it can be appreciated in Table I and Fig. 2.

We have verified that the ρ meson contribution through the ΔV_{cent} and V_{SO} terms has only minor influence on the kink. As we have explained above, this behavior is expected because the relative contributions of the ρ meson to the $(S - V)$ term, entering V_{cent} and V_{SO} , are very small.

To understand better the nature of the KE it would be useful to examine the partial contributions r_{ck} of different single-particle states "*k*" to the total charge radii r_c of the nuclei under consideration ($r_c = \sqrt{r_{c1}^2 + \dots + r_{cA}^2}$). Fig. 3 displays these values for the six bound states (closest to the Fermi level) calculated within the NL-SH model for different nuclei in the region $200 \leq A \leq 214$. We see that the total value of r_c for $A \geq 208$ is mostly determined by the contribution of the $1h_{11/2}$, $1g_{9/2}$ and $1g_{7/2}$ proton states, rather than by that of the $2d_{3/2}$, $2d_{5/2}$ or $3s_{1/2}$ proton states. Let us mention also that in the nuclei considered there are more protons of the first type than those of the second type.

Moreover, the values r_{ck} , for the states of the first type, are increasing functions of A for $A \geq 208$ while the respective values for the states of the second type almost remain constant with the increasing of A in this region. One can effectively describe this type of behavior as a result of the repulsive interaction experienced by the $1h_{11/2}$, $1g_{9/2}$ and $1g_{7/2}$ protons which pushes them outside the central part of the nucleus and increases the value of r_c . From Fig. 3 it is also seen that the behavior of the total value of r_c for the nuclei in the interval $206 \leq A \leq 208$ is strongly affected by the r_{ck} value for $k = 3s_{1/2}$. In fact, a similar influence is also shown by the $2s_{1/2}$ state, in spite of its very large binding energy. In cases where the ρ contribution to the $(S + V)$ term in the central potential is reduced (cases *b* and *d* in Fig. 2), the contributions of the two $2s_{1/2}$ and $3s_{1/2}$ states to $\Delta r_c^- = r_c(^{208}Pb) - r_c(^{206}Pb)$ are even larger. The two neutrons added to the $3p_{1/2}$ state appear to be very effective to pull on the protons in these two states.

Table I and Fig. 2 also show that in the region $206 \leq A \leq 208$ it is easier to polarize protons by adding neutrons when protons are less bound (cases *b* and *d*), in accordance with the reasons given in Ref. [5]. However, the behavior of r_c in the region $208 \leq A \leq 210$ is the opposite. The r_c behavior shows that the cases that produce larger variation of Δr_c^- are less effective contributing to $\Delta r_c^+ = r_c(^{210}Pb) - r_c(^{208}Pb)$. This is a reflection of the fact that it is more difficult to increase the r_c value by adding extra neutrons when the radius is larger than in the case when it is smaller and when the neutrons previously added are more effective to increase r_c .

As explained above, although the ρ meson contribution to the total energy is rather small in comparison with that of the σ and ω mesons, it is just the ρ meson that is mainly responsible in the RMFA for the kink structure. However, even without ρ meson contribution ($g_\rho = 0$) there is a residual kink, case *d* in Fig. 2. In this case, we have investigated the role of the different terms entering V_{cent} and of V_{SO} in producing the residual kink. To do that, we have artificially changed the contribution of these terms in a similar way as we did it for the different components of the ρ meson, but readjusting now the strength of the $(S + V)$ term, if necessary, to keep the r_c values close to the experimental ones for the *Pb* isotopes studied, (the same conditions are used for the three isotopes). These studies reveal that the terms $\varepsilon \frac{V}{M}$, ΔV_{cent} and V_{SO} contribute in a slight and positive way to the kink structure, whereas the term $(S^2 - V^2)/2M$ has an opposite effect that approximately cancels the effects mentioned above. We notice that taking about the 70% of the strength of the $(S + V)$ term entering Eq. (3) as the total potential, the KE (obtained in the *Pb* isotopes studied taking $g_\rho = 0$) is mainly reproduced as an effect of the self-consistent procedure. For example, if the S and V potentials are

approached by the Woods-Saxon functions with the radius proportional to $A^{1/3}$ the KE disappears, although different diffuseness parameters for the potentials are used.

We have studied above the role that V_{cent} and V_{SO} play in generating and forming the structure of the kink. Another crucial relativistic effect comes from the fact that the source term in the scalar field equation, the scalar density (ρ_S), is smaller than the actual baryon density (ρ_B). This difference of two densities is just the mechanism that brings about the saturation in the RMFA, and essentially distinguishes relativistic models from nonrelativistic ones. Thus it would be interesting to check also the role of this mechanism in the KE. One naive way would be to replace ρ_S in the scalar field equation by ρ_B . Since the nucleus would become unstable in this case, we add to V_{cent} in the single-particle Schrödinger equation (1) a repulsive density-dependent term formally identical to the term proportional to t_3 appearing in the corresponding equation for the Skyrme-Hartree-Fock model. The coefficient t_3 is chosen to fit the $r_c(^{208}\text{Pb})$. Under these conditions we observe that in two cases, with and without the ρ meson (cases *a* and *d*, respectively), the quantities r_c^+ and r_c^- are reduced and so is the ratio r_c^+/r_c^- . Thus, the KE is reduced about 15% in the case *a* and 60% in the case *d*. The residual KE without the ρ meson almost disappears.

Our conclusions can be summarized in the following points:

1. The KE in Pb isotopes chain appears to be a general feature of the RMFA. It is observed in both linear and nonlinear models, being more strongly manifested in the models with smaller values of K . We have found that the ρ meson plays an essential role in forming the KE. In the case without the ρ meson a small kink remains that can be attributed to relativistic as well as to self-consistent effects.

2. The KE mainly comes from the (partially) destructive interference of contributions of the ρ meson to the $(S + V)$ and $(S^2 - V^2)/2M$ components of the single-particle potential. The $(S + V)$ term leads to a KE of positive sign while the $(S^2 - V^2)/2M$ component produces a KE of negative sign. The total effect has a positive sign and corresponds to the trend observed empirically (see cases *b* and *c* in Fig. 2).

3. Excluding the ρ contribution from the two components of V_{cent} mentioned in the previous point, i.e., taking $x_1 = x_2 = 0$, one gets a strong reduction of the KE. This situation is quite similar to that in which the ρ meson contribution is completely excluded ($g_\rho=0$, case *d* in Fig. 2). The residual KE in this case is related to the self-consistent procedure. This effect completely disappears if one uses a Woods-Saxon potential in the Dirac equation rather than a self-consistent calculation.

4. The contribution of the ρ meson to V_{SO} has no influence on the KE.

5. The relativistic effect that produces saturation in the RMFA provided by the difference between the scalar density and the baryon density, also contributes to a certain increase of the KE with respect to the nonrelativistic case in which saturation is produced by a repulsive density-dependent term as in the Skyrme-Hartree-Fock model.

In a forthcoming publication we shall investigate the problem of the KE in the relativistic Hartree-Fock framework.

One of the authors (L.N.S.) is very grateful to the University of Cantabria and to the Technical University of Munich for hospitality. This work has been supported in part by the DGESIC grant PB97-0360.

REFERENCES

- [1] E.W. Otten, in: "Nuclear radii and moments of unstable nuclei", in: Treaties on heavy-ions science, ed. D.A. Bromley, Vol. 7 (Plenum, New York, 1988), p. 515.
- [2] N. Tajima, P. Bonche, H. Flocard, P.-H. Heenen, M.S. Weiss, Nucl. Phys. A551 (1993) 434.
- [3] M.M. Sharma, G.A. Lalazissis, P. Ring. Phys. Lett. **B317** (1993) 9.
- [4] M.M. Sharma, G.A. Lalazissis, J. König, P. Ring. Phys. Rev. Lett. **74** (1995) 3744.
- [5] P.G. Reinhard, H. Flocard. Nucl. Phys. **A584** (1995) 467.
- [6] P. Ring. Prog. Part. Nucl. Phys. **37** (1996) 193.
- [7] (private communication).
- [8] S. Marcos, N.V. Giai, L.N. Savushkin, Nucl. Phys. **A549** (1992) 143.
- [9] C.J. Horowitz, B.D. Serot, Nucl. Phys. **A368** (1981) 503.
- [10] M.M. Sharma, M.A. Nagarajan, P. Ring. Phys. Lett. **B312** (1993) 377.
- [11] G.A. Lalazissis, J. König and P. Ring. Phys. Rev. C **55** (1997) 540.

FIGURE CAPTIONS

Fig. 1. The charge radii of Pb isotopes obtained with the L [9], NL-SH [10] and NL3 [11] models, normalized to the experimental value of the ^{208}Pb nucleus. The empirical values (EXP) are taking from Ref. [10].

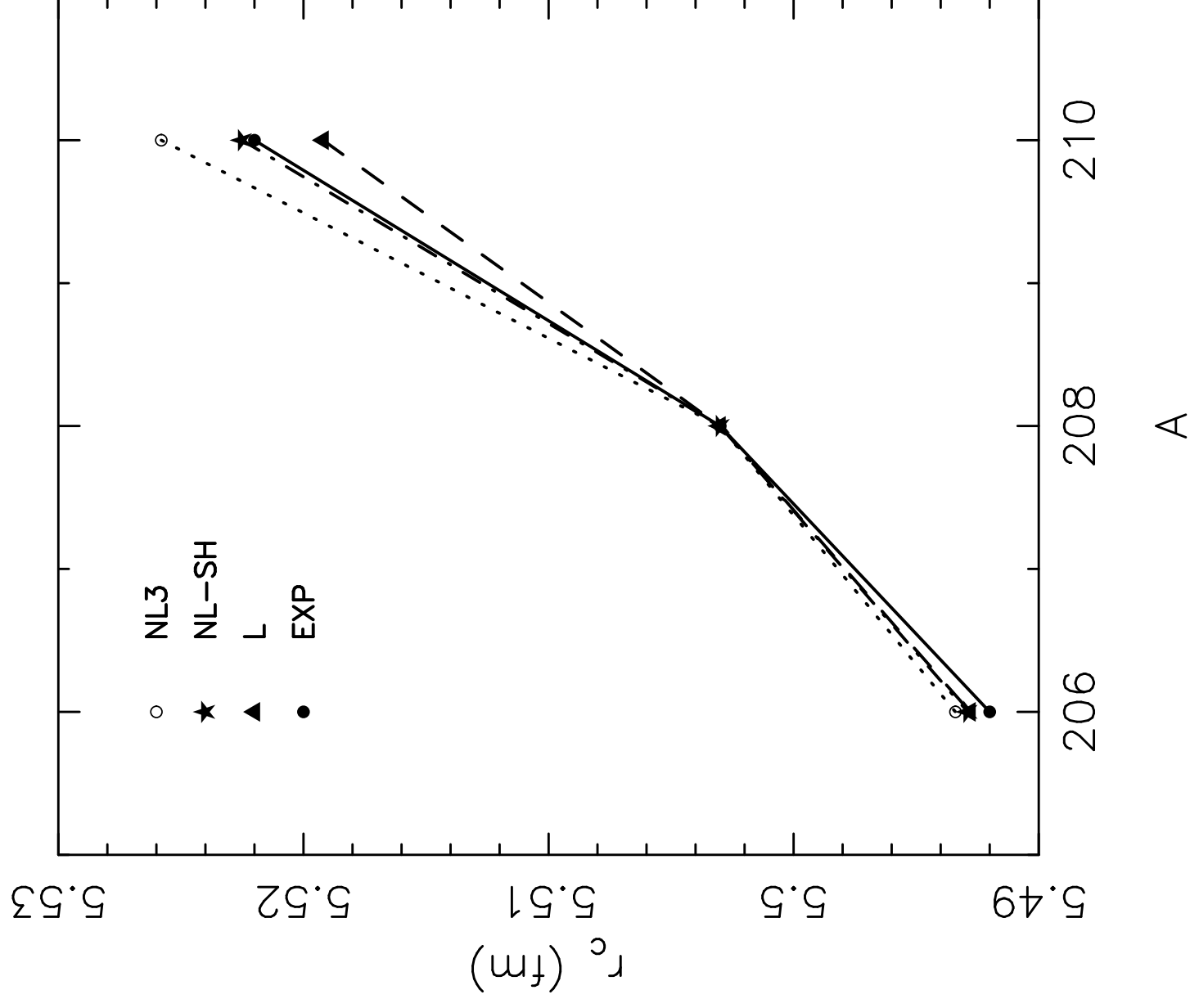
Fig. 2. The same as in Fig. 1 for the NL-SH [10] model, and the four cases considered in Table I: a : $x_{1-5} = 1$ (the exact model); b : $x_1 = 0.1$, $x_{2-5} = 1$; c : $x_{1,3-5} = 1$, $x_2 = 0$; d : $x_{1-5} = 0$ (without the ρ meson contribution).

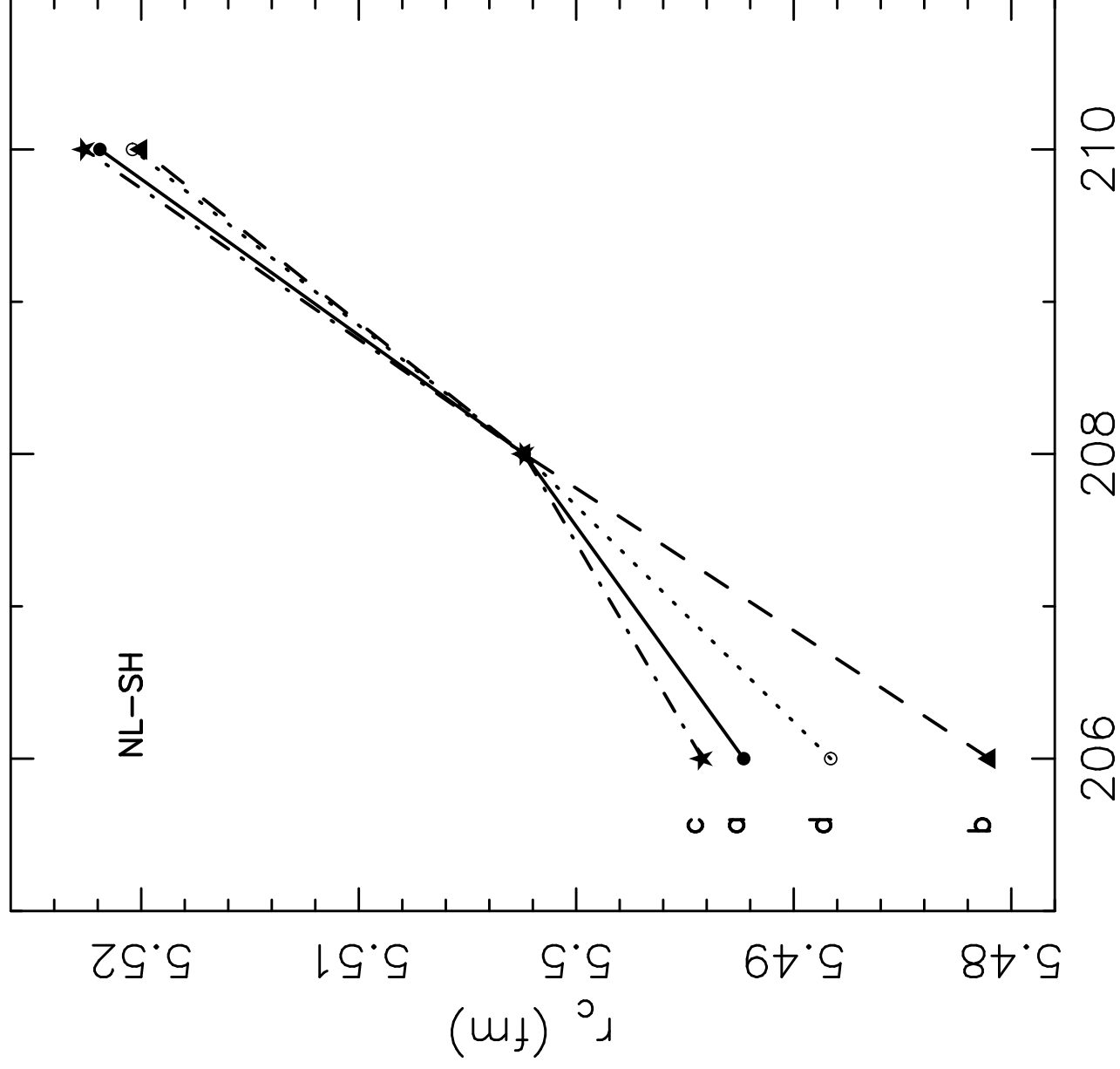
Fig. 3. The single-particle r.m.s. radii for the proton states, as indicated, in the Pb isotopes obtained with the NL-SH [10] model.

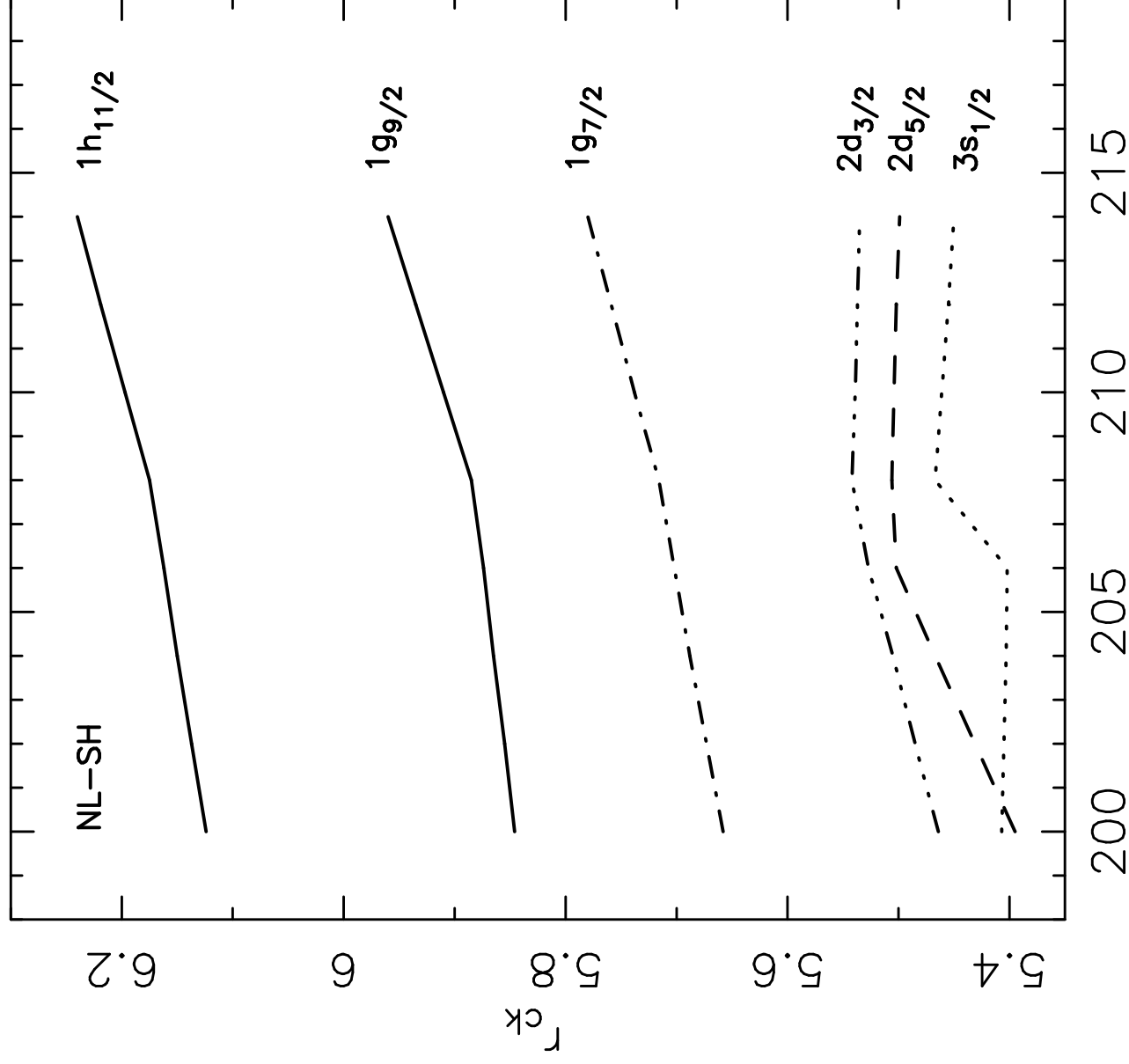
TABLES

| Model | $r_c(\text{fm})$ | $\Delta r_c^+(\text{fm})$ | $\Delta r_c^-(\text{fm})$ | $\Delta r_c^+/\Delta r_c^-$ | case |
|-------|------------------|---------------------------|---------------------------|-----------------------------|----------|
| L | 5.455 | 0.016 | 0.010 | 1.59 | <i>a</i> |
| NL-SH | 5.502 | 0.020 | 0.010 | 1.93 | <i>a</i> |
| NL3 | 5.517 | 0.023 | 0.010 | 2.37 | <i>a</i> |
| L | 5.577 | 0.016 | 0.018 | 0.88 | <i>b</i> |
| NL-SH | 5.651 | 0.018 | 0.022 | 0.82 | <i>b</i> |
| NL3 | 5.718 | 0.019 | 0.022 | 0.85 | <i>b</i> |
| L | 5.421 | 0.016 | 0.008 | 1.99 | <i>c</i> |
| NL-SH | 5.477 | 0.020 | 0.008 | 2.46 | <i>c</i> |
| NL3 | 5.495 | 0.024 | 0.008 | 3.08 | <i>c</i> |
| L | 5.510 | 0.016 | 0.014 | 1.17 | <i>d</i> |
| NL-SH | 5.558 | 0.018 | 0.014 | 1.28 | <i>d</i> |
| NL3 | 5.568 | 0.021 | 0.013 | 1.58 | <i>d</i> |
| Exp | 5.503 | 0.019 | 0.011 | 1.73 | |

TABLE I. The charge radius (r_c), $\Delta r_c^+ = r_c(^{210}\text{Pb}) - r_c(^{208}\text{Pb})$, $\Delta r_c^- = r_c(^{208}\text{Pb}) - r_c(^{206}\text{Pb})$ and the ratio $\Delta r_c^+/\Delta r_c^-$ for the linear model L [9] and the nonlinear models NL-SH [10] and NL3 [11], for the cases: *a*: $x_{1-5} = 1$; *b*: $x_1 = 0.2$ (L), 0.1 (NL-SH), 0 (NL3), $x_{2-5} = 1$; *c*: $x_{1,3-5} = 1$, $x_2 = 0$; *d*: $x_{1-5} = 0$. The last line contains the experimental results [1].







A